Dispersion engineering of photonic crystal fibers by means of fluidic infiltration

Article *in* Journal of Modern Optics · August 2012

Impact Factor: 1.01 · DOI: 10.1080/09500340.2012.715690

Journal of Modern Optics
Publication details, including instructions for authors and subscription information:
http://www.tandfonline.com/loi/tmop20

Dispersion engineering of photonic crystal fibers by means of fluidic infiltration

M. Ebnali-Heidari [a], F. Dehghan [b], H. Saghaei [b], F. Koohi-Kamali [b] & M.K. Moravvej-Farshi [c]

[a] Faculty of Engineering, University of Shahrekord, Shahrekord, 8818634141, Iran

[b] Department of Electrical Engineering, Science and Research Branch, Islamic Azad University, Tehran, 1477893855, Iran

[c] Faculty of Electrical and Computer Engineering, Advanced Device Simulation Lab, Tarbiat Modares University, PO Box 14115-194, Tehran, 1411713116, Iran

Version of record first published: 28 Aug 2012.

To cite this article: M. Ebnali-Heidari, F. Dehghan, H. Saghaei, F. Koohi-Kamali & M.K. Moravvej-Farshi (2012): Dispersion engineering of photonic crystal fibers by means of fluidic infiltration, Journal of Modern Optics, 59:16, 1384-1390

To link to this article: http://dx.doi.org/10.1080/09500340.2012.715690

Journal of Modern Optics
Vol. 59, No. 16, 20 September 2012, 1384–1390

Taylor & Francis
Taylor & Francis Group

Dispersion engineering of photonic crystal fibers by means of fluidic infiltration

M. Ebnali-Heidari[a]*, F. Dehghan[b], H. Saghaei[b], F. Koohi-Kamali[b] and M.K. Moravvej-Farshi[c]

[a]*Faculty of Engineering, University of Shahrekord, Shahrekord, 8818634141, Iran;* [b]*Department of Electrical Engineering, Science and Research Branch, Islamic Azad University, Tehran, 1477893855, Iran;* [c]*Faculty of Electrical and Computer Engineering, Advanced Device Simulation Lab, Tarbiat Modares University, PO Box 14115-194, Tehran, 1411713116, Iran*

(*Received 3 March 2012; final version received 20 July 2012*)

We present a technique based on the optofluidic method to design a photonic crystal fiber (PCF) experiencing small dispersion over a broad range of wavelengths. Without nano-scale variation in the air-hole diameter or the lattice constant of Λ, or even changing the shape of the air holes, this approach allows us to control the dispersion of the fundamental mode in a PCF simply by choosing a suitable refractive index of the liquid to infiltrate into the air holes of the PCF. Moreover, one can design a different PCF such as a dispersion flattened fiber (DFF), dispersion shifted fiber (DSF), by utilizing fluids of various refractive indices.

Keywords: photonic crystal fibers; dispersion; optofluidics

1. Introduction

In recent years, photonic crystal fibers (PCFs) have attracted a great deal of attention in various applications. One of the most promising applications of photonic crystals is the possibility of creating compact, high speed, high bandwidth, and low power integrated optical devices by means of photons as the carriers of information [1–5].

A PCF is a two-dimensional photonic crystal, possessing a central defect region surrounded by multiple air holes (tubes) devised in parallel along an optical fiber. Compared with conventional optical fibers, PCFs have unique properties [3–5], capable of being tailored to possess nearly zero dispersion. This has been recently achieved by engineering the PCF geometry, resulting in sophisticated designs that typically require nano-scale technological precision. Our focus in this paper for dispersion engineering is based on the optofluidics: a new branch in photonics that attempts to merge microfluidics and optics [6,7]. In a meticulous manner, due to their intrinsic porous nature, photonic crystal (PhC) devices infiltrated with microfluids have demonstrated tunable and reconfigurable optical properties [7–13]. Furthermore, selective liquid infiltration of individual air pores of a planar PhC lattice has shown to extend the number of opportunities associated with this optofluidic platform [14–18]. This offers the potential for realizing integrated microphotonic devices and circuits, which could be (re)configured by simply changing the liquid and/or the pattern of the infiltrated area within the PhC lattice [19–24].

There are various techniques by which the PCF can be dispersion engineered and customized for a particular application. However, most of the proposed techniques, so far, are based on varying the PCF geometry; such as varying the circular air-hole diameter (d) [25–27], the pitch size (Λ) of the periodic lattice [28], as well as the number of air-hole rings (N) surrounding the PCF core or even using ring-shaped air holes [29]. These techniques depend on the technological capability to realize a specific design with high precision, and also are limited by the size of the PCF cross-sectional area. In particular, it is quite difficult to control the accurate positions and radii of the air holes within the PCF lattice. Precision in control of these two geometrical parameters during the fabrication process in addition to the maximum number of the rings of air holes within a PCF are the most critical constraints in acquiring the desired dispersion. To overcome these topological limitations, in this paper, we numerically investigate the potential of selective optofluidic infiltration of air holes within the PCF lattice in order to tailor the fiber properties as desired. Recently, Ebnali-Heidari et al. demonstrated the dispersion engineering using optofluidic infiltration in the PhC air holes [8]. In this manner we use the same approach to engineer the dispersion of a PCF to obtain ultra-flattened dispersion curves.

*Corresponding author. Email: ebnali-m@eng.sku.ac.ir

ISSN 0950–0340 print/ISSN 1362–3044 online

http://dx.doi.org/10.1080/09500340.2012.715690
http://www.tandfonline.com

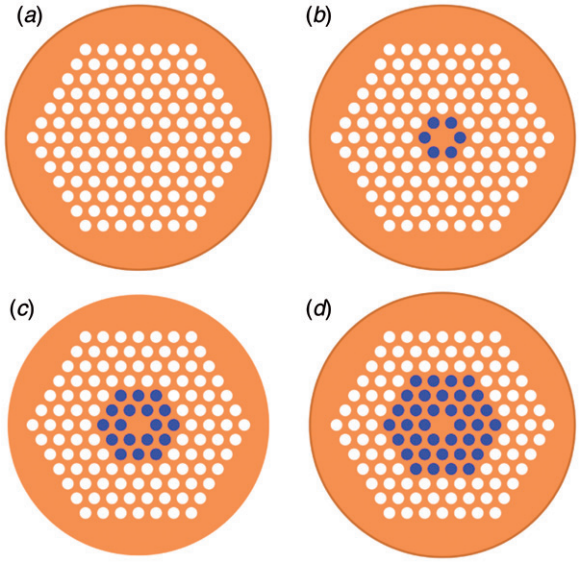

Figure 1. Cross-sectional view of four PCFs of the same lattice pitch ($\Lambda = 2\,\mu m$) and air-hole diameters ($d = 0.6\Lambda$). (*a*) Un-infiltrated, (*b*), (*c*) and (*d*) the inner most ring, the first two inner rings, and the first three inner rings all depicted by dark circles are assumed to be selectively infiltrated with an optofluidic of index n_f. (The color version of this figure is included in the online version of the journal.)

The rest of this paper is organized as follows. In Section 2, we present the procedure for dispersion engineering of solid core PCFs with triangular lattices, by means of selective optofluidic infiltration. Section 3 is dedicated to the discussion about the numerical results. Finally, we will conclude the paper in Section 4.

2. Engineering PCF dispersion by means of infiltration

The goal of this section is to investigate the possibility of tailoring the dispersion profile of a PCF as desired for designing either a dispersion shifted (DSF) fiber or a dispersion flattened fiber (DFF), by means of selective optofluidic infiltration of PCF air holes. In doing so, we have considered a solid core PCF that consists of circular air holes of diameter $d = 0.6\Lambda$ arranged in a triangular lattice of constant $\Lambda = 2\,\mu m$, as depicted in Figure 1(*a*). The air-hole lattice forms six hexagonal rings co-centered with the solid core. Figure 1(*b*) illustrates the case for which the air holes forming the inner most ring are infiltrated by an optofluidic of refractive index n_f. Figures 1(*c*) and (*d*) depict the cases for which the air holes forming the first two and the first three inner rings are selectively infiltrated, respectively. The white and dark circles in Figure 1 represent the un-infiltrated and selectively infiltrated air holes, respectively.

In order to investigate the dispersion properties of the PCF, we have employed the full-vectorial plane wave expansion (PWE) method. The dispersion is calculated by [30]:

$$D = \left(\frac{-\lambda}{c}\right)\frac{d^2 n_{eff}}{d\lambda^2}. \tag{1}$$

n_{eff} is the effective index of the fundamental mode.

The contribution of material dispersion of silica fiber in the effective index is calculated using the four-term Sellmeier formula [30].

$$n = \left(1 + \frac{0.6961663\,\lambda^2}{\lambda^2 - 0.0684043^2} + \frac{0.4079426\,\lambda^2}{\lambda^2 - 0.1162414^2} + \frac{0.8974794\,\lambda^2}{\lambda^2 - 9.896161^2}\right)^{1/2}. \tag{2}$$

Mathematically, by solving the Maxwell equation, one can relate the dispersion parameter, D, to the group velocity dispersion (GVD), β_2, as [30]:

$$D(\lambda) = \frac{d}{d\lambda}\left(\frac{1}{v_g}\right) = -\frac{2\pi c}{\lambda^2}\beta_2, \tag{3}$$

where c and λ are the light velocity and wavelength in free space, k is the corresponding wave number, and $v_g \equiv \nabla_k \omega(k)$ is the group velocity. The higher order dispersions are given by [30]:

$$\beta_m = \left.\frac{d^m \beta}{d\omega^m}\right|_{\omega=\omega_0} \tag{4}$$

in which ω_0 is the light center frequency.

In order to investigate the influence of the infiltration on the PCF dispersion properties, at first, we compare the dispersion profile for the fundamental mode of the un-infiltrated PCF of Figure 1(*a*) with those of the PCF of Figure 1(*b*) in which the most inner ring is assumed to be infiltrated with various optical fluids. Figure 2 compares the numerical results for $1.30 \le n_f \le 1.44$.

The comparison shown in Figure 2 reveals that infiltrating the most inner ring of the PCF with various optical fluids reduces the PCF dispersion value significantly and also enables one to design PCFs suitable for various applications such as dispersion flattened PCF (DF-PCF), dispersion shifted PCF (DS-PCF), and dispersion compensated PCF (DC-PCF). For example, this figure shows that the infiltration with $n_f = 1.30$ has reduced the dispersion profile, in the wavelength range of $1.05\,\mu m < \lambda < 2\,\mu m$, to insignificant values of $0 \le |D| \le 5$ (ps/km nm). This nearly flattened profile is an example of DF-PCF, over the given range of the wavelengths that makes this particular infiltrated PCF suitable for DWDM

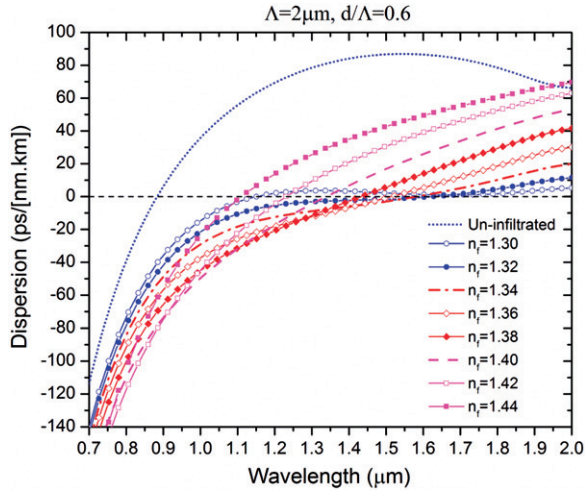

Figure 2. Comparison of the dispersion profile for the un-infiltrated PCF ($\Lambda = 2\,\mu m$ and air-hole diameters $d = 0.6\Lambda$) of Figure 1(*a*) with those of Figure 1(*b*) infiltrated with optical fluids of various indices ($1.30 \le n_f \le 1.44$). (The color version of this figure is included in the online version of the journal.)

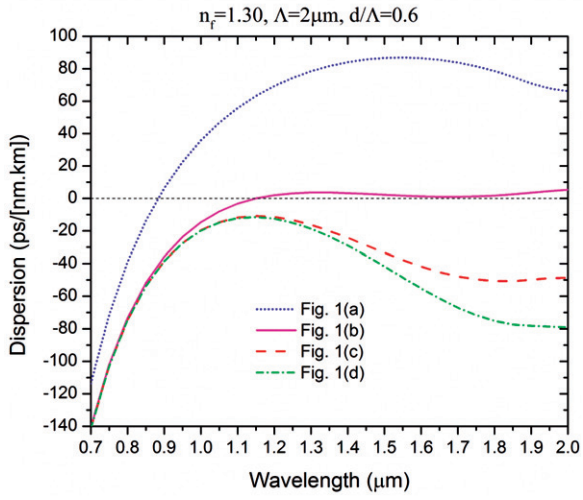

Figure 3. Comparison of the dispersion profile of the un-infiltrated PCF of Figure 1(*a*) with those of Figure 1(*b*)–(*d*) infiltrated with the optical fluid refractive index $n_f = 1.30$. (The color version of this figure is included in the online version of the journal.)

applications widely used in optical telecommunication systems. Figure 2 also shows that for infiltrations with $n_f \le 1.44$, as n_f increases the zero-dispersion wavelength experiences blue shifting at the right side, which is desirable for designing DS-PCFs.

Next, we investigate the effect of the number of infiltrated rings, as shown in Figure 1, on the PCF dispersion profile. Assuming all three PCFs shown in Figure 1(*b*)–(*d*) is infiltrated by the same optical fluid of refractive index $n_f = 1.30$, we calculated the corresponding dispersion profiles for the PCF fundamental mode. Figure 3 compares the numerical results with that of the un-infiltrated PCF of Figure 1(*a*). This comparison also shows that as the number of infiltrated rings (N) increases the dispersion profile moves toward the negative direction over the entire range of the optical communication wavelength, and making it suitable for designing the DC-PCF. Furthermore, one can observe from Figure 3 that the infiltration becomes less influential for $N > 2$, particularly on the shift on position of the zero-dispersion wavelength. This can be explained by the confinement of the fundamental in the central region of the PCF, as illustrated in Figure 4.

Instead of retracing all the steps taken during the optimization, we first illustrate the effect of varying one of the design parameters on the dispersion curve while the rest are kept constant. So we vary the size of the diameters of the air holes of the infiltrated PCF of Figure 1(*b*) with $\Lambda = 2\,\mu m$ and $n_f = 1.30$, and study the variations in the profile of the fundamental mode of the PCF and we kept constant other parameters. The numerical results are depicted in Figure 5. As compared with Figure 2, the results illustrated in this figure demonstrate that the effect of increasing the diameter size (d) is similar to the effect of decreasing the fluid refractive index. In the other words by decreasing the hole diameter, the suitable fluid to achieve a flattened dispersion profile occurred with the smaller value. This is because, the effective refractive indices of the PCFs are decreased, in both cases. To demonstrate this behavior in more detail, and also find a suitable fluid for each hole diameter to achieve a flattened dispersion profile, we plot the dispersion profile for hole diameter of $d = 1$, 1.2, 1.4, and $1.6\,\mu m$ with the infiltration of different optical fluid refractive index. Figure 6(*a*)–(*d*) reveal that for hole diameter of $d = 1$, 1.2, 1.4, and $1.6\,\mu m$, the suitable fluids of 1.28, 1.30, 1.32, and 1.34 to achieve a flattened dispersion profile are proposed.

Finally, we investigate the effect of the variation in the pitch size of the infiltrated PCF of Figure 1(*b*) with $d = 0.6\Lambda$ and $n_f = 1.30$. The numerical results, depicted in Figure 7, reveal that by increasing the PCF pitch size the flattened dispersion window is enhanced and the sign of dispersion is changed from negative to positive. This is due to the fact that an increase in Λ is similar to an increase in the fluid refractive index which is equivalent to increasing the PCF effective refractive index.

At the end to have a stronger conclusion, referring the relation between n_f, d, and lambda, by basic electromagnetic equations '$c/n = \lambda f$' for light, we can find a relation between these parameters. By the mentioned relation, it can be seen that index of

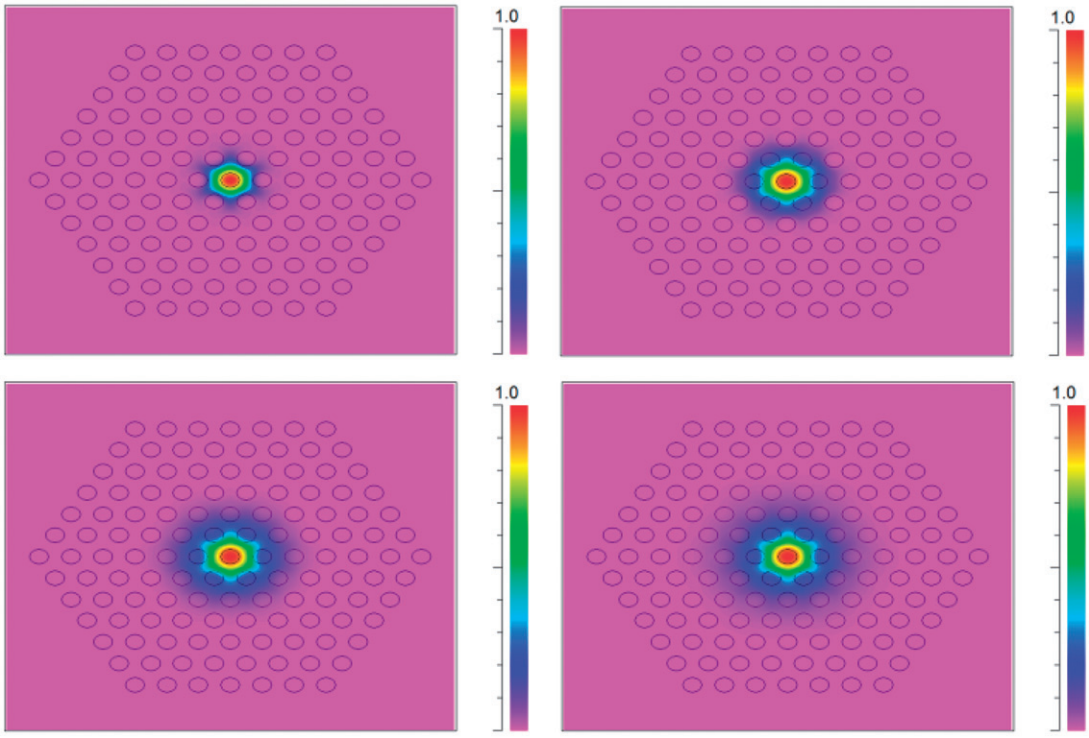

Figure 4. Comparison of the distribution of the fundamental mode of the un-infiltrated PCF of Figure 1(*a*) with those of Figure 1(*b*)–(*d*) infiltrated with the optical fluid refractive index $n_f = 1.30$. (The color version of this figure is included in the online version of the journal.)

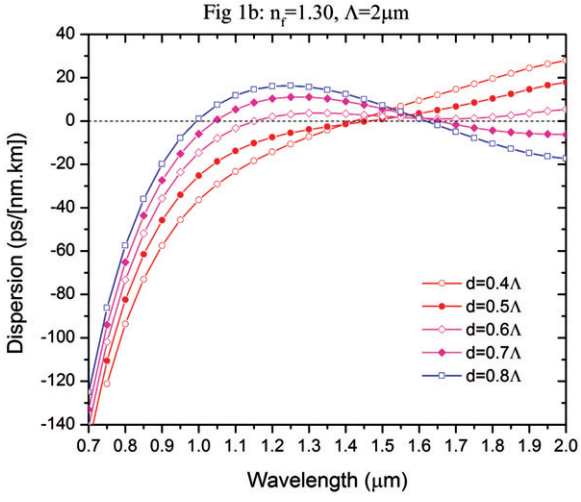

Figure 5. Effect of the variation in the size of the air-hole diameter of the infiltrated PCF of Figure 1(*b*) on the dispersion profile of its fundamental mode. (The color version of this figure is included in the online version of the journal.)

refraction and frequency are inversely related for a given wavelength of light, which supports the concept of microfluidic infiltration on the dispersion. By increasing the refractive index of the fluid, increasing the pitch value, or decreasing the hole radius, the value of the effective refractive index decreases. Consequently, for constant wavelength, the frequency value decreases. It means that the band structure of fundamental mode of the PCF shifts to the lower frequency.

The numerical results presented here, so far, show that the approach based on the selective optofluidic infiltration approach is very robust, because the deviations in hole radii from the PCF parameters targeted during the fabrication can be compensated by freely choosing the appropriate fluid refractive index, thereby making this specific dispersion engineering technique more tolerant upon the fabrication inaccuracies. As an example, a dispersion flattening can be achieved for a nominal $d/\Lambda = 0.6$ by using a fluid refractive index of 1.30 (see Figure 2(*b*)); however, if the actual hole diameter of the fabricated PCF structure deviates to $d/\Lambda = 0.5$ or 0.7, then, choosing a fluid refractive index of 1.28 and 1.32 as illustrated in Figure 8, can still provide the desirable dispersion flattened regime.

In another simulation we infiltrated only the first and third rows of ring holes of the PCF with $d = 0.6\,\Lambda$ and $n_f = 1.30$ as shown on Figure 9. It can be seen that we can achieve a wide bandwidth and very small

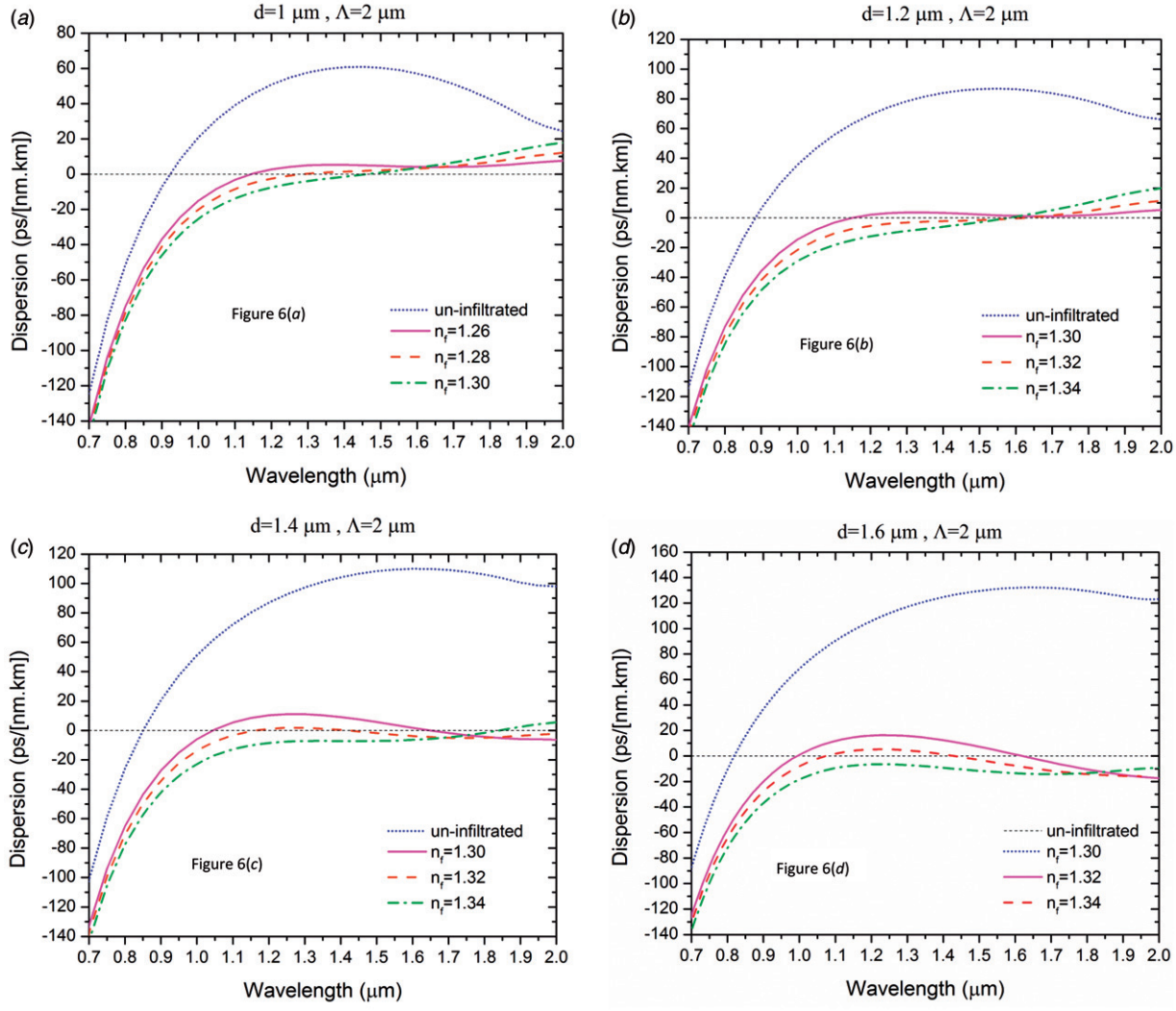

Figure 6. Comparison of the dispersion profile for the un-infiltrated PCF: (*a*) $d = 1\,\mu m$ and $\Lambda = 2\,\mu m$, (*b*) $d = 1.2\,\mu m$ and $\Lambda = 2\,\mu m$, (*c*) $d = 1.4\,\mu m$ and $\Lambda = 2\,\mu m$, (*d*) $d = 1.6\,\mu m$ and $\Lambda = 2\,\mu m$ of Figure 1(*a*) with those of Figure 1(*b*) infiltrated with the optical fluid refractive index of $n_f = 1.26$, 1.28, 1.3, 1.32, and 1.34. (The color version of this figure is included in the online version of the journal.)

dispersion; however, the infiltration process in this case is more difficult than other cases.

3. Discussion

Our engineered structure has one advantage point related to the previous engineered works based on PCF. Previous works on engineered PCF relied on the optimization of the PCF lattice geometry, where high accuracy is essential as even nanometre-scale deviations typically lead to a significant degradation in the dispersion properties. By contrast, the infiltration-based approach offers an additional and free parameter (which is independent of the fabrication) for achieving a desired dispersion. In addition, the post-process nature of this approach – the infiltration step is performed after the waveguide fabrication – allows it to be adapted depending on the actual PCF structure produced by the fabrication, while the microfluidic aspect offers the potential for (re)configuring the sensor structure at will. Considering the findings of previous studies in this area, it is argued that the dispersion is improved using nanometer variation in shape or diameter of PCF. For instance, Matsui et al. [25] and Saitoh et al. [26] obtained the dispersion and bandwidth around ± 1 ps/nm km and 400 nm, respectively, by varying the circular air-hole diameter of the PCF. Liu et al. [27] reported dispersion of ± 1 ps/nm km for 900 nm bandwidth by changing the

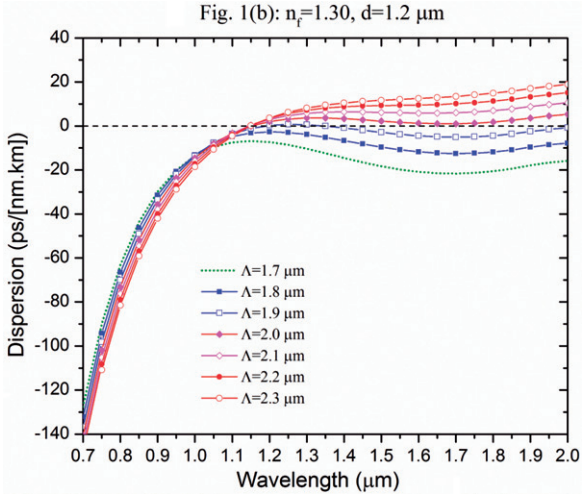

Figure 7. Effect of the variation in the pitch size of the infiltrated PCF of Figure 1(*b*) on the dispersion profile of its fundamental mode. (The color version of this figure is included in the online version of the journal.)

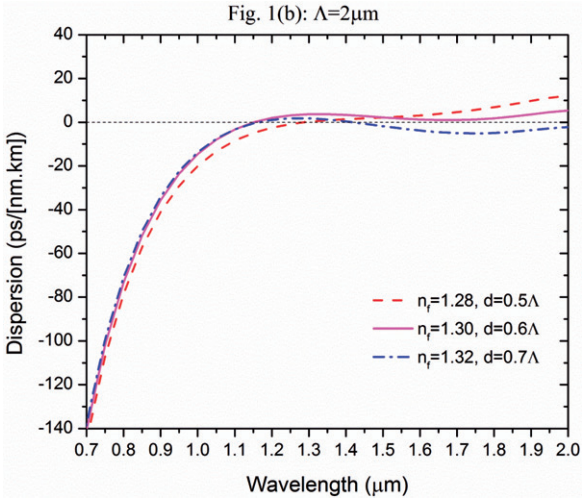

Figure 8. Dispersion profiles for PCFs of $d/\Lambda = 0.5$, 0.6, and 0.7 infiltrated with optical fluids of refractive indices 1.28, 1.30, and 1.32, respectively. (The color version of this figure is included in the online version of the journal.)

shape from circular to elliptical air holes in the PCF. From the simulation (Figures 8 and 9) it can be seen that our dispersion and bandwidth are around ±3 ps/nm km and around 1000 nm, respectively, however our dispersion engineering is based only on the optofluidics infiltration in the PCF air holes. In addition we can obtain smaller dispersion and larger bandwidth by optimizing the value of the refractive index and the number of ring infiltration.

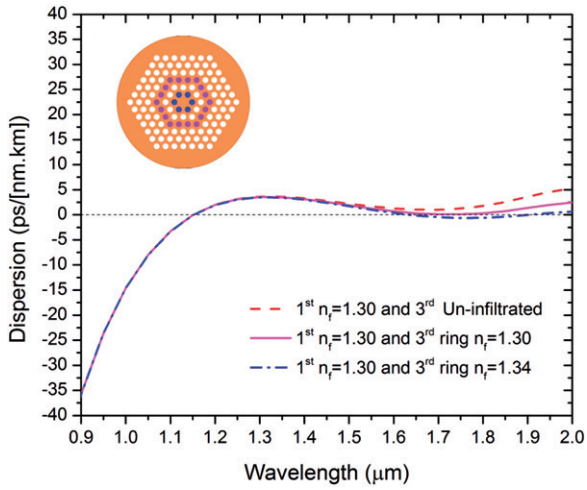

Figure 9. Dispersion profiles for PCFs with infiltration of first ring with optical fluids of refractive indices 1.30 and third ring of PCF with optical fluids of refractive indices 1.30, and 1.34. On the inset, the respective PCF waveguide geometry (with $\Lambda = 2\,\mu$m and air-hole diameters $d = 0.6\Lambda$) is shown. The dark circles are assumed to be selectively infiltrated with an optofluidic of index n_f. (The color version of this figure is included in the online version of the journal.)

4. Conclusion

A technique based on the selective liquid infiltration of triangular-lattice PCF is discussed to produce low and flattened dispersion over a substantial bandwidth. The results show that the dispersion profile is affected simply by changing the refractive index of the infiltrated liquids. For instance, modifying the value of infiltrated refractive index of the fluid for the first ring of PCF from 1.32 to 1.44 at the wavelength of 1.5 μm leads to the sign of dispersion changing and its value increases from −5 to 40 ps/km nm. We have discussed how we can design different dispersion profiles such as DSF or DFF.

References

[1] Russell, P. *Science* **2003,** *299,* 358–362.
[2] Koshiba, M.; Saitoh, K. *Opt. Lett.* **2004,** *29,* 1739–1741.
[3] Arriaga, J.; Knight, J.; Russell, P.S.J. *Phys. E (Amsterdam, Neth.)* **2003,** *17,* 440–442.
[4] Soussi, S. *Adv. Appl. Math.* **2006,** *36,* 288–317.
[5] Calo, G.; D'Orazio, A.; De Sario, M.; Mescia, L.; Petruzzelli, V.; Prudenzano, F. Photonic Crystal Fibres. In *Transparent Optical Networks*, Proceedings of 2005 7th International Conference, July 3–7, 2005; IEEE: Piscataway, NJ, 2005; Vol. 1, pp 115–120. doi:10.1109/ICTON.2005.1505764.
[6] Psaltis, D.; Quake, S.R.; Yang, C. *Nature* **2006,** *442,* 381–386.

[7] Monat, C.; Domachuk, P.; Eggleton, B. *Nat. Photon.* **2007,** *1,* 106–114.
[8] Ebnali-Heidari, M.; Grillet, C.; Monat, C.; Eggleton, B. *Opt. Express* **2009,** *17,* 1628–1635.
[9] Yoshino, K.; Shimoda, Y.; Kawagishi, Y.; Nakayama, K.; Ozaki, M. *Appl. Phys. Lett.* **1999,** *75,* 932–934.
[10] Wild, B.; Ferrini, R.; Houdre, R.; Mulot, M.; Anand, S.; Smith, C. *Appl. Phys. Lett.* **2004,** *84,* 846–848.
[11] Maune, B.; Lončar, M.; Witzens, J.; Hochberg, M.; Baehr-Jones, T.; Psaltis, D.; Scherer, A.; Qiu, Y. *Appl. Phys. Lett.* **2004,** *85,* 360–362.
[12] Yu, C.; Liou, J.; Huang, S.; Chang, H. *Opt. Express* **2008,** *16,* 4443–4451.
[13] Sharkawy, A.; Pustai, D.; Shi, S.; Prather, D.; McBride, S.; Zanzucchi, P. *Opt. Express* **2005,** *13,* 2814–2827.
[14] Erickson, D.; Rockwood, T.; Emery, T.; Scherer, A.; Psaltis, D. *Opt. Lett.* **2006,** *31,* 59–61.
[15] Intonti, F.; Vignolini, S.; Türck, V.; Colocci, M.; Bettotti, P.; Pavesi, L.; Schweizer, S.L.; Wehrspohn, R.; Wiersma, D. *Appl. Phys. Lett.* **2006,** *89,* 2111171–2111173.
[16] Smith, C.L.C.; Wu, D.K.C.; Lee, M.W.; Monat, C.; Tomljenovic-Hanic, S.; Grillet, C.; Eggleton, B.J.; Freeman, D.; Ruan, Y.; Madden, S. *Appl. Phys. Lett.* **2007,** *91,* 1211031–1211033.
[17] Bog, U.; Smith, C.L.C.; Lee, M.W.; Tomljenovic-Hanic, S.; Grillet, C.; Monat, C.; O'Faolain, L.; Karnutsch, C.; Krauss, T.F.; McPhedran, R.C. *Opt. Lett.* **2008,** *33,* 2206–2208.
[18] Smith, C.L.; Bog, U.; Tomljenovic-Hanic, S.; Lee, M.W.; Wu, D.K.; O'Faolain, L.; Monat, C.; Grillet, C.; Krauss, T.F.; Karnutsch, C. *Opt. Express* **2008,** *16,* 15887–15896.
[19] Bitarafan, M.; Moravvej-Farshi, M.; Ebnali-Heidari, M. *Appl. Opt.* **2011,** *50,* 2622–2627.
[20] Bakhshi, S.; Moravvej-Farshi, M.K.; Ebnali-Heidari, M. *Appl. Opt.* **2011,** *50,* 4048–4053.
[21] Bakhshi, S.; Moravvej-Farshi, M.K.; Ebnali-Heidari, M. *Appl. Opt.* **2012,** *51,* 2687–2692.
[22] Mingaleev, S.F.; Schillinger, M.; Hermann, D.; Busch, K. *Opt. Lett.* **2004,** *29,* 2858–2860.
[23] Kurt, H.; Citrin, D.S. *Opt. Express* **2008,** *16,* 11995–12001.
[24] Ferrando, A.; Silvestre, E.; Andres, P.; Miret, J.J.; Andres, M.V. *Opt. Express* **2001,** *9,* 687–697.
[25] Matsui, T.; Nakajima, K.; Sankawa, I. *J. Lightwave Technol.* **2007,** *25,* 757–762.
[26] Saitoh, K.; Koshiba, M.; Hasegawa, T.; Sasaoka, E. *Opt. Express* **2003,** *11,* 843–852.
[27] Liu, Z.; Liu, X.; Li, S.; Zhou, G.; Wang, W.; Hou, L. *Opt. Commun.* **2007,** *272,* 92–96.
[28] Shen, L.; Huang, W.P.; Chen, G.; Jian, S. *IEEE Photon. Technol. Lett.* **2003,** *15,* 540–542.
[29] Park, M.; Arabi, H.E.; Lee, S.; Oh, K. *Opt. Commun.* **2011,** *284,* 4914–4919.
[30] Agrawal, G. *Nonlinear Fiber Optics*, 3rd ed.; Academic Press: New York, 2001.